PROGRESS IN BIOMEDICAL OPTICS

Proceedings of

Photodynamic Therapy: Mechanisms II

Thomas J. Dougherty
Chair/Editor

Abraham Katzir
Biomedical Optics Series Editor

16–17 January 1990
Los Angeles, California

Sponsored by
SPIE—The International Society for Optical Engineering

Published by
SPIE—The International Society for Optical Engineering
P.O. Box 10, Bellingham, Washington 98227-0010 USA

SPIE P PROCEEDINGS SERIES

SPIE Volume 12(

The papers appearing in this book comprise the proceedings of the meeting mentioned on the cover and title page. They reflect the authors' opinions and are published as presented and without change, in the interests of timely dissemination. Their inclusion in this publication does not necessarily constitute endorsement by the editors or by SPIE.

Please use the following format to cite material from this book:
Author(s), "Title of Paper," *Photodynamic Therapy: Mechanisms II,* Thomas J. Dougherty, Editor, Proc. SPIE 1203, page numbers (1990).

Library of Congress Catalog Card No. 90-60142
ISBN 0-8194-0244-3

Published by
SPIE—The International Society for Optical Engineering
P.O. Box 10, Bellingham, Washington 98227-0010 USA
Telephone 206/676-3290 (Pacific Time) • Fax 206/647-1445

Printed in the United States of America.

CONFERENCE COMMITTEE

Biomedical Optics Symposium Chair
Abraham Katzir, Tel Aviv University (Israel)

Conference Chair
Thomas J. Dougherty, Roswell Park Memorial Institute

Session Chairs
Session 1—Tumor Detection/Tissue Optical Properties/Dosimetry
Daniel R. Doiron, LaserTherapeutics, Inc.

Session 2—Tissue Targeting of Photosensitizers
Tayyaba Hasan, Wellman Laboratories of Photomedicine,
Harvard Medical School and Massachusetts General Hospital

Session 3—Tissue Effects/New Photosensitizers
Steven H. Selman, M.D., Medical College of Ohio

Session 4—New Photosensitizers
Alan R. Morgan, University of Toledo

Conference 1203, *Photodynamic Therapy: Mechanisms II*, was part of a four-conference SPIE Symposium on Biomedical Optics held at OE/LASE '90, 14–19 January 1990, Los Angeles, California. The other conferences were:

Conference 1200, *Laser Surgery: Advanced Characterization, Therapeutics, and Systems II*
Conference 1201, *Optical Fibers in Medicine*
Conference 1202, *Laser-Tissue Interaction.*

Symposium Chair: **Abraham Katzir,** Tel Aviv University (Israel)

INTRODUCTION

Photodynamic therapy is rapidly maturing both as a clinically useful modality and as a new branch of photobiology. While to date all clinical data have been obtained using the porphyrin oligomeric mixtures Hpd or Photofrin II, numerous potentially improved photosensitizers are in various phases of preclinical studies. As we learn more about the in-vivo action of the porphyrins, particularly relating to vascular changes, direct cellular effects, release of various cytokines, and even induction of certain cellular genes, it is clear that not all sensitizers will behave similarly. For example, hydrophilicity is important but clearly not sufficient for useful in-vivo action. Further, certain disulfonated phthalocyanines show vastly different properties depending on how the charge is distributed over the molecule with the more amphiphilic isomers being the superior in-vivo sensitizers. It also appears that certain of the newer sensitizers will not produce the prolonged cutaneous photosensitivity inherent in the current porphyrin materials. It now appears likely that photosensitizers absorbing near 800 nm will be developed, thus allowing for optimum tissue penetration as well as use of simpler light delivery sources, i.e., diode lasers.

The future of this modality is not limited only to cancer therapy, where all clinical emphasis has been to date, but may also have application in cleansing the blood supply of viruses and in treatment of venereal warts and other virus-induced lesions. It seems clear that in one form or another PDT will be around for some time to come.

Thomas J. Dougherty
Roswell Park Memorial Institute

PHOTODYNAMIC THERAPY: MECHANISMS II

Volume 1203

CONTENTS

(continued)

PHOTODYNAMIC THERAPY: MECHANISMS II

Volume 1203

PHOTODYNAMIC THERAPY: MECHANISMS II

Volume 1203

SESSION 1

Tumor Detection/Tissue Optical Properties/Dosimetry

Chair
Daniel R. Doiron
LaserTherapeutics, Inc.

OPTICAL CHARACTERISTICS OF INTRAOCULAR TUMORS IN THE VISIBLE AND NEAR INFRARED

Lars O. Svaasand[*], Elisa Morinelli[¤], Charles J. Gomer[¤] and A. Edward Profio[#]

[*]University of Trondheim, N-7034, Norway,
[¤]Clayton Ocular Oncology Center Childrens Hospital of Los Angeles and University of Southern California School of Medicine, Los Angeles. CA 90027
[#]University of California, Santa Barbara

ABSTRACT

The optical properties of neoplastic and normal tissues have been evaluated in the wavelength region from red to near infrared. The tumor models have been human retinoblastoma and B16 melanotic melanoma transplanted in athymic mice and mammary adenocarcinoma in C3H mice. The normal tissue results include in vivo measurements in human and rabbit muscle.

2. INTRODUCTION

During recent years several new modalities for the treatment of neoplastic tissues have been evaluated. The use of lasers in the therapy of intraocular tumors may represent interesting possibilities for non-invasive treatments. The pertinent light tissue interaction may either be of thermal character or it may be based on a photochemically induced cytotoxic action such as in the case of photodynamic therapy.

The transmission spectrum of human ocular media, which covers the wavelength region from about 400 nm to 1200 nm, exhibits maximum transmission of more than 90% in the red/near infrared region 600-900 nm. The transmission in the 900-1200 nm region has a dip to about 40% at 950-1000 nm together with a peak value of about 80% at 1100 nm. The transmission deteriorates with age due to enhanced scattering and formation of a yellowish pigmentation of the lens. This pigmentation will, together with the fact that the scattering efficiency usually increases somewhat with decreasing wavelength, further tend to suppress the transmission in the violet/blue region compared to that of the red/near infrared region.

The commonly utilized photosensitizer in photodynamic therapy has been hematoporphyrin derivative. This sensitizer can be efficiently excited at 630 nm wavelength. But recent development of new photosensitizers such as phthalocyanines and chlorins, indicates that compounds with absorption in the wavelength region

of 650-800 nm may be of clinical relevance in the near future.
The development of technology for optical fiber telecommunication systems has fortunately resulted in a wide range of high power solid state laser sources in the near infrared region. Recent development of high power GaAlAs diodes has resulted in laser diodes with emission in the wavelength region from 750 nm to 904 nm with continuously emitted power in the order of 1-3 W. As a result of this development of the diode technology stable, miniaturized diode pumped Nd:YAG lasers have equally become commercially available.

3. THEORY

The detailed calculation of light propagation in highly scattering and inhomogeneous media such as most tissues, is very complex. An exact solution of the fundamental electromagnetic equations renders an impossible task because such a solution would require detailed information of the optical properties of all local structures in the tissue.
Therefore, several approximate analytical and numerical mathematical models are being applied. Among these models are the Monte Carlo model, models based on the classical Boltzmann transport equation, the Kubelka-Munk model and several models based on optical diffusion theory.[1-6]
The Monte Carlo model is a numerical method based on computer tracking of individual photons; the computer basically follows each photon through a large number of scattering events.
The Boltzmann transport equation is in principle an analytical model which calculates the number of photons lost from the direction of beam propagation due to absorption and scattering together with accounting for the number of photons being scattered back into this particular direction through multiple scattering. In practice, however, only approximate numerical solutions of the Boltzmann equation are obtainable.
The Kubelka-Munk method is a one dimensional model of heuristic structure. In the most simplified version two diffuse photon fluxes are being considered; one flux propagating in the forward direction and the other flux in the backward direction. The spatial variations of these two fluxes are assumed to be caused by either absorption or by scattering between the fluxes.
The diffusion theory, which can be derived through a series expansion of the more general transport equations, is valid when the light is scattered to an almost isotropic distribution. A net flux of diffuse photons is then anticipated to flow from regions with high optical fluence rate to regions with lower fluence rate. This flow occurs in a manner similar to the situation when heat flows from a high temperature region to surrounding locations with lower temperatures.

In the case of broad beam irradiation of semi-infinite tissues the optical fluence rate can be approximated,

$$\phi = \phi_o \exp(-x/\delta) \qquad \text{Eq.1}$$

where x is the distance from the exposed surface. The optical fluence rate, i.e. the quantity of light irradiated onto an infinitesimally small sphere divided by the cross-sectional area of that sphere, is given by ϕ. The optical penetration depth is given by δ. This parameter is dependent on both the scattering and the absorption properties of the tissue. In tissues with very little scattering, such as in the case of ocular media, the penetration depth is approximately equal to the reciprocal absorption coefficient. In most tissues, however, where the scattering coefficient is much larger than the absorption coefficient, the penetration depth is approximately proportional to the reciprocal geometric mean value of the scattering and the absorption coefficient. The parameter ϕ_o expresses the fluence rate at the surface.

When a collimated beam is irradiating onto a tissue with negligible scattering the surface fluence rate is given by,

$$\phi_o = (1-\Gamma_s) I_o \qquad \text{Eq.2}$$

where Γ_s and I_o are, respectively, the specular reflection coefficient and the power density of the incident beam.

In a highly scattering medium the incident beam will be scattered into a diffuse, isotropic light distribution at the surface layer. The large back-scattering will enhance the optical fluence rate in the surface layer. When the surface of a highly scattering tissue is irradiated with a non-collimated isotropic irradiation the surface fluence rate becomes,

$$\phi_o = 2(1+\Gamma_d) I_o \qquad \text{Eq.3}$$

where Γ_d is the diffuse reflection coefficient.

The diffuse reflection coefficient is significantly higher than the specular reflection coefficient. The diffuse reflection coefficient for red and near-infrared irradiation is in the case of non-pigmented tissues, typically one order of magnitude larger than the specular coefficient. Since this diffuse reflection coefficient is in the range Γ_d= 0.2-0.5, it follows that the fluence rate in the surface layer may be up to 2-3 times larger than the incident irradiation.

4. RESULTS

The 425-900 nm transmission spectra of whole human blood are shown in fig.1. The samples were irradiated with a broad beam from a quartz-halogen lamp and the transmitted light was measured with a 275 cm focal length spectrograph equipped with a 1024 element intensified diode array. Figures 1a and 1b show, respectively, the transmission spectra of 0.1 mm and 1 mm thick layers. The two absorption peaks of oxyhemoglobin around 540 nm and 580 nm, which are clearly distinguishable in the 0.1 mm thick sample, are hardly seen in the 1 mm thick sample. The 1 mm sample exhibit, however, a marked absorption maximum around 760 nm. This absorption peak corresponds simultaneously to a small absorption peak in deoxygenated hemoglobin and to a weak water absorption peak at 754 nm wavelength.[7)]

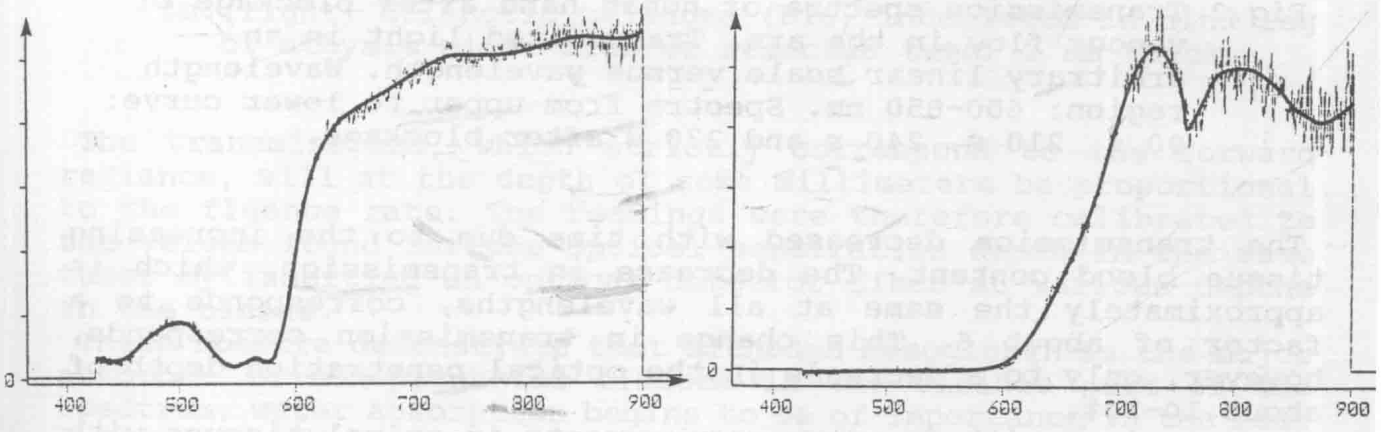

Fig.1 Spectral transmission of whole human blood.
Transmitted light in an arbitrary linear scale versus wavelength. Wavelength region: 425-900 nm.
1a.(left) Transmission through a 0.1 mm thick layer.
1b.(right) Transmission through a 1 mm thick layer.

The in vivo transmission spectrum of the human hand is shown in fig.2. The four different curves show the transmission versus time after blockage of the venous return flow in the arm.

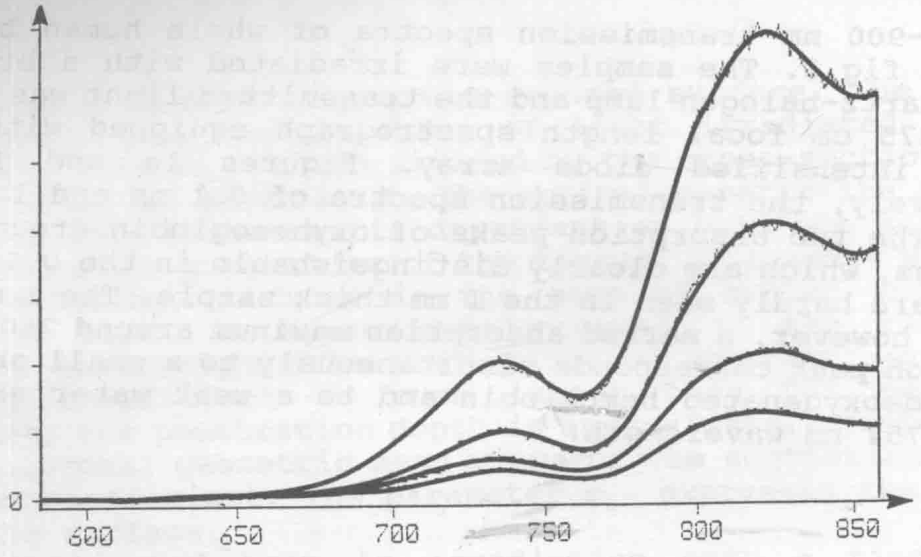

Fig.2 Transmission spectra of human hand after blockage of venous flow in the arm. Transmitted light in an arbitrary linear scale versus wavelength. Wavelength region: 600-850 nm. Spectra from upper to lower curve: 90 s, 210 s, 240 s and 270 s after blockage.

The transmission decreased with time due to the increasing tissue blood content. The decrease in transmission, which is approximately the same at all wavelengths, corresponds to a factor of about 6. This change in transmission corresponds, however, only to a decrease in the optical penetration depth of about 10-20%.

A comparison with in vitro measurements in animal tissues with varying blood content indicated that the value of 10-20 % corresponds to the typical dependence of the optical penetration depth on blood content. Further on, comparison between in vivo results and measurements after sacrifice of the animal indicated that the optical penetration depth remain the same provided that the blood remains in the tissue.

The spectral transmission through a non-pigmented tumor is shown in fig.3a. The tumor was a human retinoblastoma heterotransplanted in the thigh muscle of athymic mice. The figure shows the 450-900 nm transmission measured in vitro through a 12 mm thick slab of tumorous tissue. The corresponding results in the case a heavily pigmented tumor are shown in fig.3b. This pigmented sample was a 2 mm thick slab of B16 melanotic melanoma. This tumor was also inoculated in the thigh muscle of athymic mice.

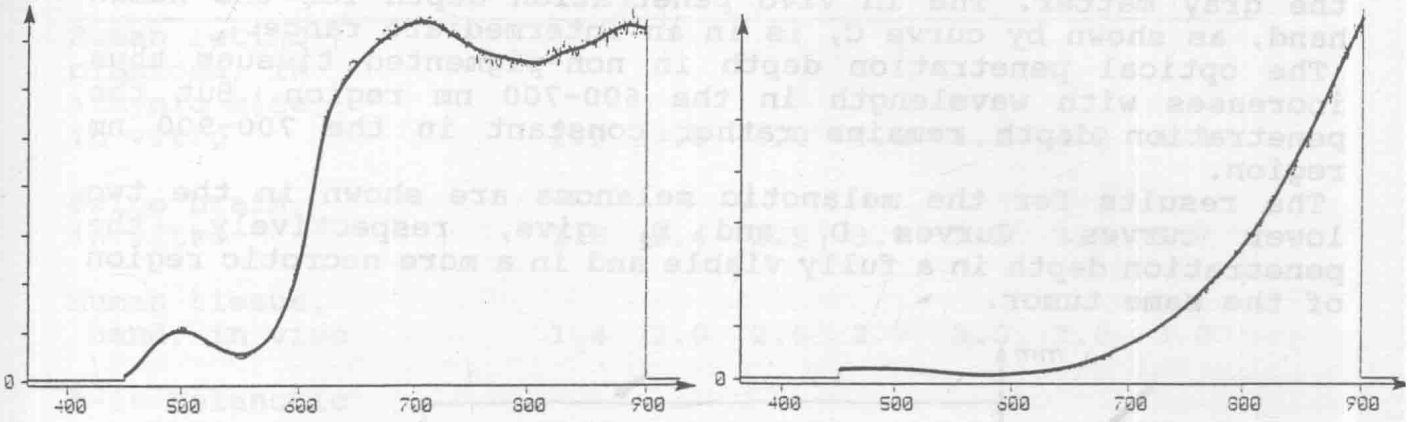

Fig.3 Spectral transmission in ocular tumor models. Transmitted light in an arbitrary linear scale versus wavelength. Wavelength region: 450-900 nm.
3a. (left) Human retinoblastoma inoculated in hind leg of athymic mice. Slab of resected tumor 12 mm thick.
3b. (right) Melanotic melanoma (B16) inoculated in hind leg of athymic mice. Slab of resected tumor 2 mm thick.

The transmissions, which strictly correspond to the forward radiance, will at the depth of some millimeters be proportional to the fluence rate. The readings were therefore calibrated to the values found for the optical penetration depth in the same tumor by inserting an optical detector fiber at various depths in the tissue.[7)]

These spectra demonstrate that although hemoglobin is the major absorber in non-pigmented tissues in the visible part of the spectrum, water absorption begins to be of importance in the near infrared spectrum. The transmission minimum at about 760 nm is for example also seen in highly scattering aqueous media with no hemoglobin content.

The optical transmission in melanotic melanoma revealed that, although hemoglobin may contribute somewhat to the attenuation in the 500-600 nm region, melanin is the dominant absorber. The optical penetration depth was in this tumor model found to increase almost exponentially with wavelength. The overall value for the optical penetration depth in the 700-900 nm region was in this case found to be almost one order of magnitude smaller than for the case of the retinoblastoma.

The results for the 600-900 nm wavelength region are summarized in fig.4.[7)] The vertical axes shows the optical penetration depth in a logarithmic scale versus wavelength. The curve A gives the penetration depth in a non-pigmented tissue with relatively limited scattering such as in the case of the retinoblastoma. The curves B_1 and B_2 give, respectively, the penetration depth in

gray matter and in white matter of swine brain. The penetration depth in the white matter is, due to the enhanced scattering in this type of tissue, significantly smaller than in the case of the gray matter. The in vivo penetration depth for the human hand, as shown by curve C, is in an intermediate range.

The optical penetration depth in non-pigmented tissues thus increases with wavelength in the 600-700 nm region. But the penetration depth remains rather constant in the 700-900 nm region.

The results for the melanotic melanoma are shown in the two lower curves. Curves D_1 and D_2 give, respectively, the penetration depth in a fully viable and in a more necrotic region of the same tumor.

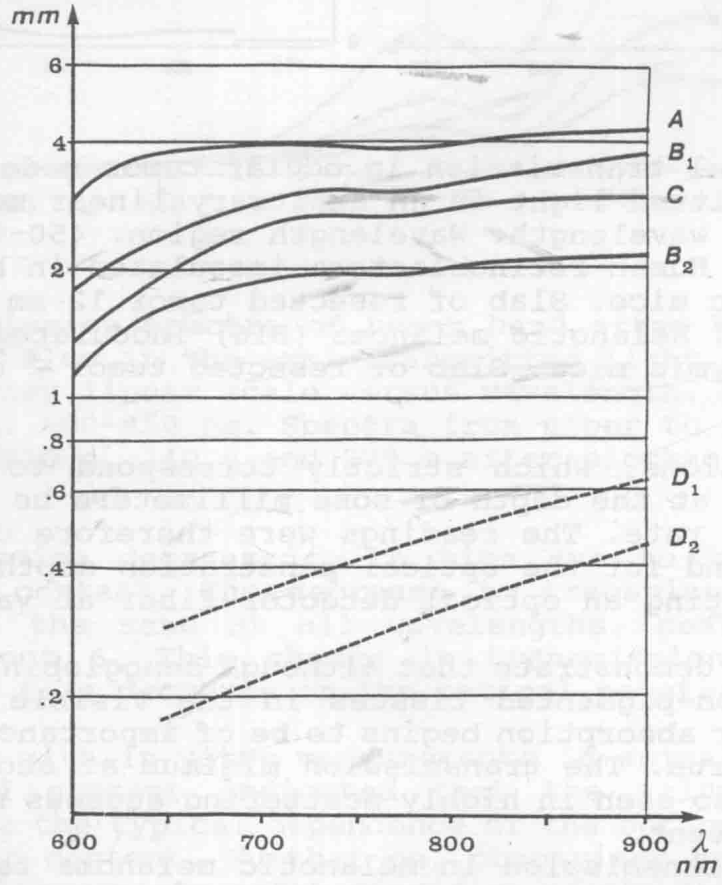

Fig.4 Optical penetration depth for various tissues in the near infrared wavelength region of 600-900 nm.
Curve A : Retinoblastoma, in vitro
Curve B_1: Gray matter of swine brain, in vitro
Curve B_2: White matter of swine brain, in vitro
Curve C : Human hand, in vivo
Curve D_1: Melanotic melanoma, viable tumor, in vivo and in vitro.
Curve D_2: Melanotic melanoma, necrotic tumor, in vivo and in vitro.

Tissue	Wavelength in nm						
	600	650	700	750	800	850	900
Human retino-blastoma, in athymic mice, in vitro	2.9	3.8	4.0	4.0	4.1	4.2	4.3
Swine brain, in vitro	1.8	2.4	2.9	3.0	3.3	3.5	3.7
Human tissue, ,hand, in vivo	1.4	2.0	2.6	2.7	3.0	3.0	3.0
B-16 Melanotic melanoma, in athymic mice, in vivo	-	0.28	0.34	0.41	0.50	0.56	0.64

Tissue	Wavelength in nm				
	633	753	816	834	1064
Human retino-blastoma in athymic mice, in vitro	3.7	4.0	4.2	4.2	5.1
Mammary adeno-carcinoma in C3H mice, in vivo :	-	2.5	-	2.7	4.1
Thigh muscle, pigmented rabbit, in vivo:	-	3.0	3.7	4.1	6.2
B-16 melanotic melanoma in athymic mice, in vivo					
viable tumor :	-	0.42	0.50	0.50	1.4
necrotic region :	-	0.26	0.34	0.36	1.2

Table 1. Optical penetration depth δ in mm.
1a.(upper) Measured with quartz-halogen lamp and spectrometer.
1a.(lower) Measured with GaAlAs and Nd:YAG lasers and fiber detectors.

Results for the red and near infrared properties of various tissues are given in table 1. Table 1a gives the calibrated results as determined from the measurements with the quartz-halogen lamp and the spectrometer whereas table 1b gives the corresponding values determined with laser sources and inserted optical detector fiber.

5. DISCUSSION

The red and near infrared properties of non-pigmented tissues are characterized by scattering and by absorption in hemoglobin and water. The maximum transmission is found in tissues with low pigmentation and scattering such as retinoblastoma and rabbit muscle. The optical penetration depth in these tissues increases with wavelength from about δ=3 mm at 600 nm to δ=4 mm at 700 nm whereas the value remains more constant in the near infrared region from 750 nm to 900 nm.

The corresponding values in non-pigmented highly scattering tissues such as in the white matter of the brain, are about 50% less.

The optical properties of pigmented tumors are more strongly wavelength dependent. The penetration depth in melanotic tumors is approximately exponentially dependent on the wavelength. The value at a wavelength of 900 nm is typically twice as large as the corresponding value at 700 nm. The penetration depths in melanotic tumors are, however, significantly smaller than in the case of non-pigmented tissues. The penetration depth at 800 nm wavelength in a melanotic tumor is about 10% of the corresponding value for the retinoblastoma.

This highest values for the penetration depth are found at 1064 nm wavelength. Typical values for non-pigmented tissues are in this case in the range δ=4-6 mm whereas the corresponding values for melanotic tissues are in the range δ=1-1.5 mm.

6.ACKNOWLEDGEMENTS

The assistance of I.Schjetne and I.Gravlien is acknowledged. The work has in part been supported by grants from the Royal Norwegian Council for Scientific and Industrial Research and from Fokus bank, Trondheim. The work was performed in conjunction with the Clayton Foundation for Research and supported in part by USPHS Grant CA-44733 awarded by the National Cancer Institute, NIH.